ORIGINAL RESEARCH

MAP2K2 Delays Recovery in Murine Models of Acute Lung Injury and Associates with Acute Respiratory Distress Syndrome Outcome

Ke-Qin Gong[1], Carmen Mikacenic[1,2], Matthew E. Long[1,3], Charles W. Frevert[1,4], Timothy P. Birkland[1], Jean Charron[5], Sina A. Gharib[1], and Anne M. Manicone[1]

[1]Division of Pulmonary, Critical Care and Sleep Medicine, and [4]Department of Comparative Medicine, University of Washington, Seattle, Washington; [2]Benaroya Research Institute, Seattle, Washington; [3]Division of Pulmonary, Critical Care and Sleep Medicine, the Ohio State University Wexner Medical Center, Columbus, Ohio; and [5]Oncology Division, Quebec University Hospital Center–Laval University Research Center, Laval University Research Center and Department of Molecular Biology, Medical Biochemistry and Pathology, Laval University, Quebec City, Quebec, Canada

Abstract

Acute respiratory distress syndrome (ARDS) remains a significant problem in need of new pharmaceutical approaches to improve its resolution. Studies comparing gene expression signatures in rodents and humans with lung injury reveal conserved pathways, including MAPK (mitogen-activated protein kinase)/ERK (extracellular signal-related protein kinase) activation. In preclinical acute lung injury (ALI) models, inhibition of MAP2K1 (MAPK kinase 1)/MAP2K2 (MAPK kinase 2) improves measures of ALI. Myeloid cell deletion of MAP2K1 results in sustained MAP2K2 activation and nonresolving ALI, suggesting that MAP2K2 deactivation may be a key driver of ALI resolution. We used human genomic data from the iSPAAR (Identification of SNPs Predisposing to Altered Acute Lung Injury Risk) Consortium to assess genetic variants in MAP2K1 and MAP2K2 for association with mortality from ARDS. To determine the role of MAP2K2 in ALI recovery, we studied mice deficient in *Map2k2* (*Mek2*$^{-/-}$) and wild-type control mice in ALI models. We identified a MAP2K2 variant that was associated with death in ARDS and MAP2K2 expression. In *Pseudomonas aeruginosa* ALI, *Mek2*$^{-/-}$ mice had similar early alveolar neutrophilic recruitment but faster resolution of alveolar neutrophilia and vascular leak. Gene expression analysis revealed a role for MAP2K2 in promoting and sustaining select proinflammatory pathway activation in ALI. Bone marrow chimera studies indicate that leukocyte MAP2K2 is the key regulator of ALI duration. These studies implicate a role for MAP2K2 in ALI duration via transcriptional regulation of inflammatory programming with potential relevance to ARDS. Targeting leukocyte MAP2K2 may be an effective strategy to promote ALI resolution.

Keywords: *Pseudomonas aeruginosa*; pneumonia; MEK1; MEK2

Clinical Relevance

These studies implicate a role for MAP2K2 in acute lung injury duration via transcriptional regulation of inflammatory programming with potential relevance to acute respiratory distress syndrome. Targeting MAP2K2 may be an effective strategy to promote acute lung injury resolution.

(Received in original form June 2, 2021; accepted in final form December 30, 2021)

Supported by National Heart, Lung, and Blood Institute grant R01 HL144656 (A.M.M.), Cystic Fibrosis Foundation Postdoc-to-Faculty Transition Award LONG19F5 (M.E.L.), Cystic Fibrosis Foundation research grant MANICO19G0 (A.M.M.), and University of Washington Cystic Fibrosis Research Development Program grant SINGH19R0 (C.W.F.).

Author Contributions: K.-Q.G. performed experiments and analyzed data. C.M. provided and analyzed data from the iSPAAR case-control study. M.E.L. performed experiments and analyzed data. C.W.F. analyzed and scored histology. T.P.B. performed experiments. J.C. provided mice. S.A.G. analyzed RNA sequencing data. A.M.M. conceived of the idea and analyzed data. A.M.M. initially drafted the manuscript, and all authors edited and approved the final version.

Correspondence and requests for reprints should be addressed to Anne M. Manicone, M.D., Center for Lung Biology, University of Washington, 850 Republican Street, Seattle, WA 98109. E-mail: manicone@u.washington.edu.

This article has a related editorial.

This article has a data supplement, which is accessible from this issue's table of contents at www.atsjournals.org.

Am J Respir Cell Mol Biol Vol 66, Iss 5, pp 555–563, May 2022

Originally Published in Press as DOI: 10.1165/rcmb.2021-0252OC on February 14, 2022
Internet address: www.atsjournals.org

Acute respiratory distress syndrome (ARDS) is a clinical disease marked by respiratory failure caused by disruption of the epithelial and endothelial barrier, flooding of the alveolar compartment with protein-rich fluid, and recruitment of neutrophils into the alveolar space (1, 2). It affects approximately 200,000 patients annually in the United States and results in approximately 75,000 deaths. In the setting of the current pandemic of severe acute respiratory syndrome coronavirus 2 infection, the incidence of ARDS has been increasing (3), and there is an urgent need to further understand its pathobiology to develop novel therapeutics (4–6). Studies comparing rodent and human lung injury gene expression signatures reveal conserved pathways (7, 8), including MAPK (mitogen-activated protein kinase) and ERK (extracellular signal-related kinase) activation during injury. In preclinical models of acute lung injury (ALI), inhibition of MAP2K1 (MAPK kinase 1)/MAP2K2 (MAPK kinase 2) improves measures of ALI (9–11).

MAP2K1 (MEK1) and MAP2K2 (MEK2), which have conserved functions across eukaryotes, participate in intracellular signaling networks and exert control on the downstream effector molecules ERK1 and ERK2 (ERK1/2) via MAP2K1 and MAP2K2 (MEK1/2)–dependent serine and tyrosine phosphorylation (12). The MAP2K–ERK1/2 pathway can be stimulated by extracellular stimuli, such as growth factors and cytokines, and signal downstream of Ras and Raf (12). Abnormal regulation of these pathways has been reported across diseases, including cancer, cardiovascular disease, and pulmonary diseases such as asthma, emphysema, and ARDS (13–17). More recently, immune-related targets of MAP2K pathways have been described. For example, the MAP2K pathway promotes proinflammatory macrophage polarization (18, 19), and MAP2K inhibitors reduce inflammation and multiorgan dysfunction in a murine model of sepsis (20). In our studies, we found that MAP2K pathways inhibit M2 (IL-4) polarization, and deactivation of the MAP2K pathway promotes a switch from inflammatory to reparative macrophage function (9, 10).

MAP2K1 and MAP2K2 share 80% amino acid identity, suggesting that they may be functionally redundant. In certain cases, deletion of both isoforms is required for phenotypes to emerge (21). However, MAP2K2-deficient (*Mek2*$^{-/-}$) mice are phenotypically normal, whereas MAP2K1 deletion is embryonic lethal, suggesting that MAPK cascade signaling is dependent on select isoforms in specific settings (22). Despite their homology, only MAP2K1 contains an inhibitory domain that can be phosphorylated by ERK1/2 in a negative feedback loop (23). We and others have demonstrated sustained activation of MAP2K2 in MAP2K1-deleted cells, suggesting that MAP2K1 is required to deactivate MAP2K2 (24–26). Myeloid deletion of MAP2K1 leads to prolonged activation of the MAP2K2-ERK1/2 axis, with sustained inflammatory responses and nonresolving lung injury (25). On the basis of these findings, we hypothesized that MAP2K2 activation would be detrimental to ALI recovery. In this study, we initially examined *MAP2K1* and *MAP2K2* single nucleotide polymorphisms (SNPs) SNPs for their associations with ARDS mortality. Next, we investigated the role of MAP2K2 in murine models of ALI using *Mek2*$^{-/-}$ mice.

Methods

Genetic Association

We obtained genomic data from the iSPAAR (Identification of SNPs Predisposing to Altered Acute Lung Injury Risk) Consortium (27). Additional details on this cohort and genotyping are provided in the data supplement. We selected SNPs in *MAP2K2* and *MAP2K1* considering directly genotyped polymorphisms within $\pm$2 kb of these genes. SNPs were removed for a call rate $<$90%, a minor allele frequency $<$5%, and a Hardy-Weinburg equilibrium *P* value of less than 0.001. This resulted in seven SNPs in *MAP2K2* and nine SNPs in *MAP2K1* that were carried forward for analyses. Among subjects with ARDS, these individual SNPs were tested for association with 28-day mortality using multiple logistic regression assuming additive genetic effects. We adjusted for age, sex, presence of sepsis, Acute Physiology and Chronic Health Evaluation III scores, and the first three principal components calculated using genome-wide data. We corrected for multiple hypothesis testing using the Bonferroni method.

Mice

Mek2$^{-/-}$ and wild-type (WT) mice (129/SvEv), a gift of Dr. Jean Charron, were generated as previously described (28). *Mek2*$^{-/-}$ and WT control mice between 8 and 12 weeks of age of both sexes were used for all experiments. Mice were bred and maintained in a specific pathogen–free facility at the University of Washington. The Institutional Animal Care and Use Committee at the University of Washington reviewed and approved all animal procedures described in these studies. Mouse genotyping was performed as reported in the data supplement.

Lung Injury Models

For the LPS-ALI model, mice were anesthetized using isoflurane, and PBS containing 1.5 mg/kg *Escherichia coli* LPS (50 μl) was instilled into the lung by oropharyngeal aspiration. For the infectious ALI model, 1.25–2.5 $\times$ 10^6 cfu of *Pseudomonas aeruginosa* (PA) strain K 50 μl was delivered via oropharyngeal aspiration. Mice were monitored and weighed daily. On Days 2–4 after infection, mice were euthanized by intraperitoneal delivery of Beuthanasia-D and harvested for BAL and lung tissue.

Chimera Generation

See the data supplement for details regarding methods for generating bone marrow chimera mice.

BAL and Lung Processing

See the data supplement for details regarding methods for BAL and lung processing.

ALI Scoring

Histological assessment of lung inflammation and injury was completed using formalin-fixed, paraffin-embedded lung tissue stained with hematoxylin and eosin. Semiquantitative histopathology scoring was performed by a comparative pathologist (C.W.F.). Additional detail on the scoring method is provided in the data supplement.

Western Blots

Processing of lung digest or BAL cells for protein and Western blots are as described in the data supplement. Antibodies used for Western blotting are listed in Table E2 in the data supplement.

RNA Sequencing

See the data supplement for details regarding processing and analysis. All RNA sequencing data meeting Minimum Information About

Table 1. Clinical Characteristics of Patients with Acute Respiratory Distress Syndrome

Characteristic	Alive (*n* = 820)	Dead (*n* = 241)
Age, yr, mean ± SD	53.7 ± 17.0	65.4 ± 15.6
Male sex, *n* (%)	464 (57)	135 (56)
Sepsis, *n* (%)	556 (68)	198 (82)
APACHE III score, mean ± SD	79.9 ± 25.7	101.3 ± 26.3

Definition of abbreviation: APACHE = Acute Physiology and Chronic Health Evaluation.

a Next-Generation Sequencing Experiment guidelines have been deposited at the Gene Expression Omnibus repository (GSE175580).

Statistics

Statistical analyses were performed using GraphPad Prism 8 software. Samples were analyzed using Student's *t* test or ANOVA for multiple comparisons, as noted in individual figure legends. For data not normally distributed, Mann-Whitney or Kruskal-Wallis tests were used. Significance was considered as $P < 0.05$.

Results

MAP2K2 SNP Associates with Death in Patients with ARDS

Studies comparing gene expression signatures in rodents and humans with lung injury reveal MAPK/ERK activation (7, 8). In our studies, we found activation of the MAPK/ERK pathway in alveolar macrophages from patients with ARDS (25). Given these findings, we evaluated SNPs in *MAP2K1* and *MAP2K2* for association with ARDS susceptibility and ARDS mortality using the iSPAAR cohort. In the 1,061 subjects with ARDS, 28-day mortality was 23% (Table 1). Subjects who died were older on average, had a higher proportion of sepsis, and had higher Acute Physiology and Chronic Health Evaluation III scores. The overall cohort had a slight male predominance.

We found an SNP in *MAP2K2* that was associated with mortality. Each copy of the minor allele of rs350912A was associated with increased odds of 28-day mortality (odds ratio, 1.53; 95% confidence interval, 1.19–1.97; Bonferroni-corrected $P = 0.006$; Table 2). This intronic SNP is a *cis*-expression quantitative trait locus for *MAP2K2* gene expression in multiple tissues and is associated with increased expression (29). No other polymorphism in *MAP2K1* or *MAP2K2* was associated with ARDS mortality (Tables 2 and 3). These results show that genetic variation within the *MAP2K2* gene is associated with an increased risk of death in ARDS.

Mek2$^{-/-}$ Mice Have Accelerated Resolution of Lung Injury Associated with Reduced Phosphorylated ERK Activation

To test the contribution of MAP2K2 in ALI, we obtained mice deficient in *Map2k2* (*Mek2*$^{-/-}$) and studied the inflammatory and injury responses to an infectious model of lung injury. *Mek2*$^{-/-}$ and WT mice were challenged with PA via oropharyngeal aspiration, and we measured daily weight as a surrogate marker of illness severity. PA-infected *Mek2*$^{-/-}$ and WT mice lost similar amounts of weight between Days 0 and 2. Weight loss among PA-infected *Mek2*$^{-/-}$ mice stabilized by Day 3 and showed improvement by Day 4, compared with sustained weight loss in WT mice (Figure 1A). Mice were killed at Days 2 and 4 to assess the inflammatory and injury responses during induction of lung injury and the start of its resolution.

On Day 2, BAL cell counts increased similarly in both genotypes (Figure 1B), with most of these cells representing neutrophils (Figure 1C). By Day 4, the BAL cell counts were lower in PA-treated *Mek2*$^{-/-}$ mice compared with WT mice (Figure 1B), and this reduction was owing to fewer BAL neutrophils (polymorphonuclear leukocytes) (Figure 1C). Vascular leak, as measured by BAL total protein and IgM, was also similarly increased at Day 2 compared with Day 0 in both infected genotypes (Figures 1E and 1F). However, by Day 4, vascular injury markers were significantly reduced in *Mek2*$^{-/-}$ compared with WT mice, indicating faster resolution of ALI (Figures 1E and 1F). Consistent with the cell count and vascular leak data, lung histopathology demonstrated reduced tissue inflammation and lung injury scores at Day 4 in *Mek2*$^{-/-}$ mice compared with WT mice (Figure 1G). Day 2 bacterial counts from the lung as measured by cfu/g were similar between WT and *Mek2*$^{-/-}$ mice (Figure 1H). By Day 4, clearance of bacteria was slightly faster in *Mek2*$^{-/-}$ mice (Figure 1H). To determine if the faster resolution of ALI was dependent on differences in bacterial clearance, we examined the inflammatory response using

Table 2. SNPs in *MAP2K2* Tested for Association with Mortality in Acute Respiratory Distress Syndrome

SNP	Major Allele	Minor Allele	MAF	Feature	*P* Value	OR (95% CI)	Bonferroni-corrected *P* Value
rs350912	G	A	0.29	Intron	0.0009	1.53 (1.19–1.97)	0.006
rs350887	G	A	0.21	Intron	0.05	1.32 (1.00–1.74)	0.36
rs350886	C	T	0.34	3′ UTR	0.11	1.21 (0.96–1.54)	0.77
rs350897	C	T	0.44	Intron	0.40	0.91 (0.72–1.14)	1
rs350896	G	A	0.48	Intron	0.93	1.01 (0.80–1.27)	1
rs4525614	G	A	0.05	Intron	0.37	1.27 (0.75–2.15)	1
rs12459940	T	C	0.28	Intron	0.25	0.86 (0.67–1.11)	1

Definition of abbreviations: CI = confidence interval; MAF = minor allele frequency; *MAP2K2* = mitogen-activated protein kinase kinase 2; OR = odds ratio; UTR = untranslated region.
P values were adjusted for age, sex, sepsis, APACHE III score, and the first three principal components with Bonferroni-adjusted *P* values for seven hypothesis tests.

Table 3. SNPs in *MAP2K1* Tested for Association with Mortality in Acute Respiratory Distress Sundrome

Predictor	Major Allele	Minor Allele	Feature	MAF	*P* Value	OR (95% CI)	Bonferroni-corrected *P* Value
rs7166547	C	T	5′ UTR	0.17	0.13	1.25 (0.94–1.67)	1
rs1549854	A	C	5′ UTR	0.47	0.99	0.99 (0.80–1.26)	1
rs4489951	A	G	5′ UTR	0.09	0.64	0.91 (0.61–1.36)	1
rs1432443	A	C	5′ UTR	0.33	0.67	0.95 (0.74–1.21)	1
rs1432442	C	T	5′ UTR	0.09	0.25	1.26 (0.85–1.86)	1
rs1432441	G	A	Intron	0.33	0.67	0.95 (0.74–1.21)	1
rs12050732	A	C	Intron	0.17	0.12	1.26 (0.95–1.68)	1
rs4255740	C	T	Intron	0.33	0.66	0.95 (0.74–1.21)	1
rs12594835	T	C	Intergenic	0.33	0.66	0.95 (0.74–1.21)	1

P values were adjusted for age, sex, sepsis, APACHE III score, and the first three principal components with Bonferroni-adjusted *P* values for nine hypothesis tests.

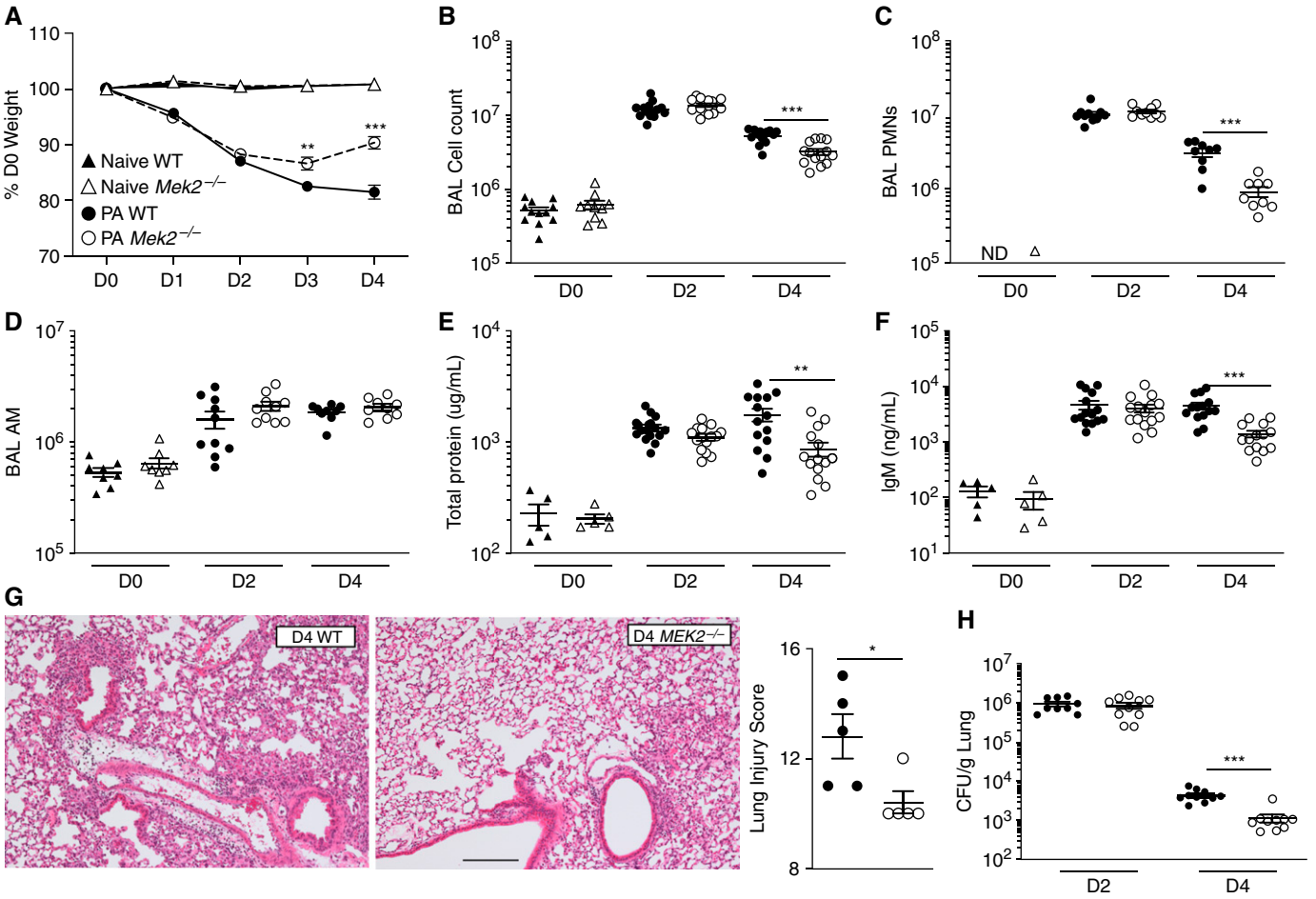

Figure 1. MAP2K2 (mitogen-activated protein kinase kinase 2) deletion leads to faster *Pseudomonas aeruginosa* (PA) acute lung injury (ALI) resolution. Mice received PA via oropharyngeal aspiration and were harvested at Day (D) 2 and D4. Naive mice (D0) were used as control animals. (*A*) PA wild-type (WT) mice had continued weight loss between D0 and D4, whereas PA mice deficient in Map2k2 (*Mek2*$^{-/-}$) recovered weight faster than WT mice at D3 and D4. (*B*) BAL cell counts and (*C*) BAL neutrophils (polymorphonuclear leukocytes [PMNs]) were similar at D0 and D2 between genotypes but reduced in *Mek2*$^{-/-}$ mice compared with WT mice at D4. (*D*) Alveolar macrophages (AMs) increased in PA-infected mice, with no difference by genotype. (*E*) BAL total protein and (*F*) IgM were similarly increased at D2 in both genotypes but reduced in *Mek2*$^{-/-}$ mice by D4. Analysis was performed using one-way ANOVA, and data are presented as mean ± SEM ($n = 5$–15/group). (*G*) Representative lung sections stained with hematoxylin and eosin from D4 demonstrate increased inflammatory cells in WT mice (left) compared with *Mek2*$^{-/-}$ mice (right) with quantitative scoring of lung injury. Scale bar, 100 μm. (*H*) Bacterial cfu/g of lung at D2 and D4. Analysis was performed using Student's *t* test, and data are presented as mean ± SEM ($n = 5$–10/group). *$P < 0.05$, **$P < 0.01$, and ***$P < 0.001$. CFU = colony-forming unit.

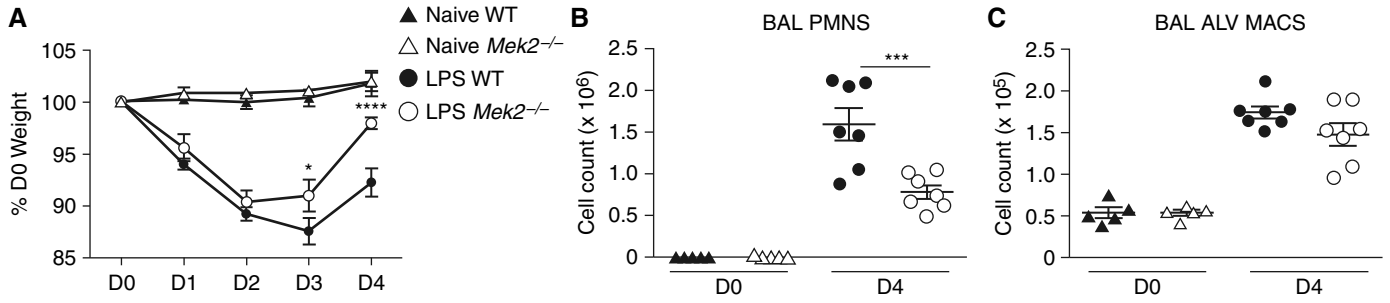

Figure 2. MAP2K2 deletion leads to faster recover from LPS ALI. Mice received *Escherichia coli* LPS via oropharyngeal aspiration and were harvested at D4. Naive mice (D0) were used as control animals. (*A*) LPS *Mek2*$^{-/-}$ mice had earlier recovery of total body weight compared with LPS WT mice at D3 and D4. (*B*) BAL neutrophils (PMNs) were not present at D0 and were reduced at D4 in *Mek2*$^{-/-}$ mice compared with WT mice. (*C*) AMs increased in LPS-treated mice, with no difference by genotype. Analysis was performed using ANOVA, and data are presented as mean ± SEM (n = 5–7/group). *P < 0.05, ***P < 0.001, and ****P < 0.0001. ALV MACS = alveolar macrophages.

E. coli LPS as a sterile model of lung injury. We found a similar protective effect in *Mek2*$^{-/-}$ mice, characterized by faster recovery of total body weight and reduced BAL neutrophilia at Day 4, compared with similarly treated WT mice (Figure 2).

Because MAP2K2 activates ERK1/2 via threonine and tyrosine phosphorylation, we quantified phosphorylated ERK1/2 (p-ERK) protein concentrations in protein isolated from lung digest (Figure 3A) and BAL cells (Figure 3B). In both the lung and BAL compartments, p-ERK1/2/ERK concentrations were lower in *Mek2*$^{-/-}$ compared with WT mice at Day 2 after infection, indicating that MAP2K2 is necessary for ERK activation in ALI. We also observed reduced p-ERK1/2/ERK concentrations in *Mek2*$^{-/-}$ compared with WT mice at Day 4 (data not shown), indicating that MAP2K2 regulates sustained p-ERK1/2 activation in ALI. MAP2K2 protein was undetectable in *Mek2*$^{-/-}$ mice (not shown), and MAP2K1 concentrations were unaffected by deletion of MAP2K2 (Figures 3A and 3C).

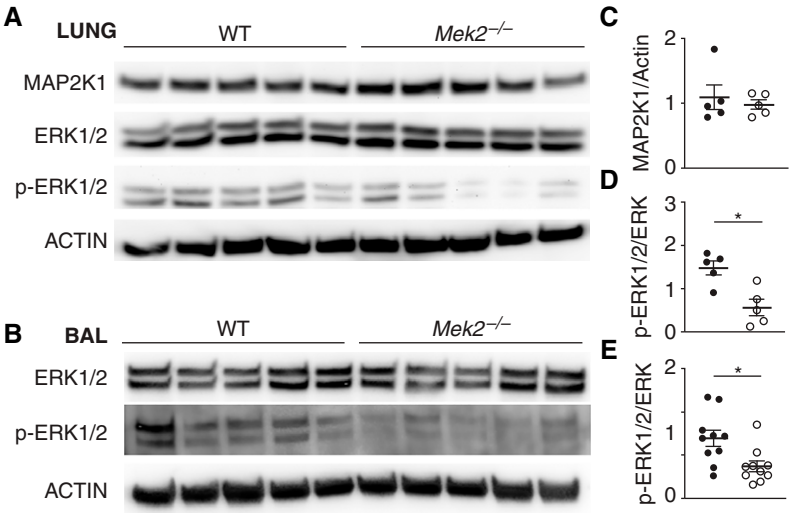

Figure 3. MAP2K2 sustains ERK1/2 (extracellular signal-related kinase 1 and 2) activation in PA ALI. (*A* and *B*) Protein from lung digests (*A*) and BAL cells (*B*) was analyzed for expression of MAP2K1 (mitogen-activated protein kinase kinase 1), ERK1/2, phosphorylated ERK1/2 (p-ERK1/2), and β-actin at D2 after infection in WT (solid circles) and *Mek2*$^{-/-}$ (open circles) mice. (*C*) MAP2K1 concentrations were unaffected by deletion of MAP2K2. (*D* and *E*) p-ERK1/2 concentrations in the (*D*) lung and (*E*) BAL were significantly reduced in the absence of MAP2K. Analysis was performed using Student's *t* test, and data are presented as mean ± SEM (n = 5-10/genotype). *P < 0.05.

MAP2K2 Regulates IFN, Immunoinflammatory, and Repair Pathways in ALI

To determine how MAP2K2 may be driving altered inflammatory and repair processes in ALI, we analyzed lung tissue for gene expression using RNA sequencing during naive state (Day 0) and at Days 2 and 4 after infection. Principal-component analysis of the entire gene expression data (~16,800 genes) demonstrated separation between genotypes across time points, indicating distinct transcriptional profiles between WT and *Mek2*$^{-/-}$ mice during the course of PA lung infection (Figure 4A). As expected, compared with baseline (Day 0), there was widespread alteration in gene expression at Day 2 (WT, 5,240 genes; *Mek2*$^{-/-}$, 4,131 genes) and Day 4 (WT, 4,322 genes; *Mek2*$^{-/-}$, 1,226 genes). However, *Mek2*$^{-/-}$ mice had fewer differentially expressed genes relative to baseline, particularly by Day 4. To assess the role of *Map2k2* in regulating the transcriptional response to PA infection, differential gene expression was compared on the basis of genotype at each time point. Few genes were different between WT and *Mek2*$^{-/-}$ at Day 0 (n = 53, false discovery rate < 0.01), with the most significant gene being *Map2k2* (false discovery rate = 2.43×10^{-38}). By Day 2 after infection, 512 genes were differentially expressed between WT and *Mek2*$^{-/-}$ mice, and by Day 4, the number had further increased to 1,798 genes (Figure 4B). This finding highlights a MAP2K2-driven divergence in pulmonary gene expression response to PA infection. To better understand the processes

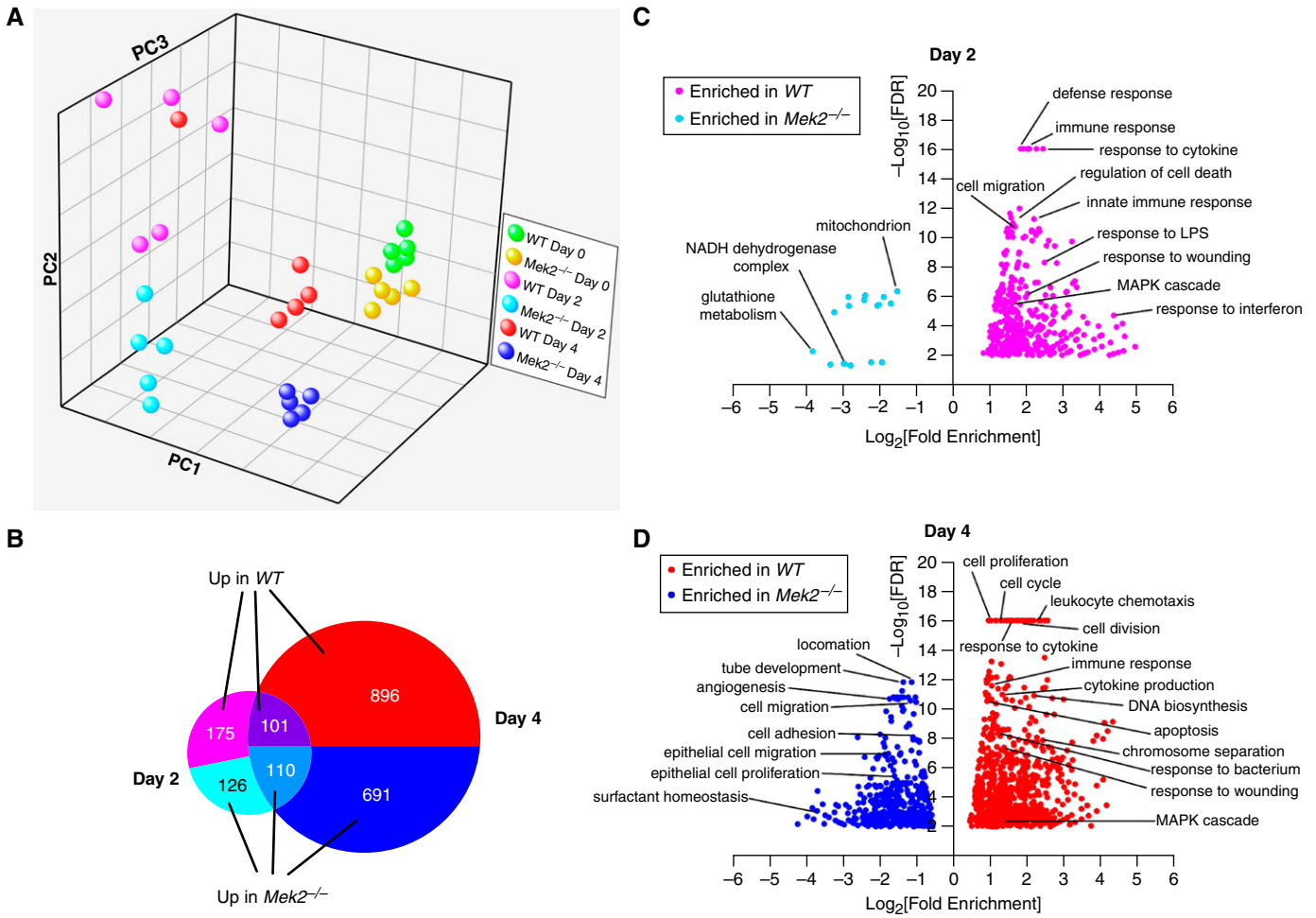

Figure 4. MAP2K2 enhances inflammatory programming in ALI. (*A*) Principal-component analysis of the entire gene expression data demonstrates genotype and time-dependent clustering. (*B*) Graphical representation of up- and downregulated genes between genotypes at D2 and D4. (*C* and *D*) Volcano plots representing enriched pathways in WT and *Mek2*$^{-/-}$ lungs at D2 (*C*) and D4 (*D*). By D4, reparative processes were highly enriched in lungs from *Mek2*$^{-/-}$ mice, whereas WT animals were characterized by continued enrichment of proinflammatory pathways as well as cell cycle/division and apoptotic processes. FDR = false discovery rate; MAPK = mitogen-activated protein kinase; NADH = nicotinamide adenine dinucleotide reduced; PC = principal component.

differentially regulated by MAP2K2, we performed functional enrichment analysis on the differentially expressed genes between WT and *Mek2*$^{-/-}$ mice at Day 2 and Day 4. As summarized in Figure 4C, WT mice had higher enrichment of immunoinflammatory, interferon, and apoptotic programs at Day 2 compared with *Mek2*$^{-/-}$ mice. By Day 4, reparative processes were highly enriched in *Mek2*$^{-/-}$ mice, whereas WT animals were characterized by continued enrichment of proinflammatory pathways as well as cell cycle/division and apoptotic processes (Figure 4D). Overall, these findings indicate that MAP2K2 is critical for activation and persistence of injurious pathways in PA pneumonia.

MAP2K2 in the Leukocyte Compartment Regulates Duration of ALI

To determine the cellular source of MAP2K2 responsible for the observed phenotypes in *Mek2*$^{-/-}$ (knockout [KO]) mice, we generated bone marrow chimeras (Figure 5). After 12 weeks, mice were exposed to PA and killed on Day 4 to assess BAL cell counts, cell differential, and colony-forming units in the lung tissue. By tracking daily weight, we observed the expected earlier recovery of total body weight in KO/KO compared with WT/WT mice (Figure 5A). WT mice that received KO bone marrow (WT/KO) also recovered their total body weight faster, similar to the result observed in KO/KO chimeras (Figure 5A). However, the weight change in KO/WT mice more closely resembled that of WT/WT mice. The changes in BAL neutrophils also reflected these genotype-dependent differences, with WT/KO and KO/KO mice having fewer BAL neutrophils and reduced lung colony-forming units compared with WT/WT and KO/WT groups (Figures 5B and 5D). Macrophage numbers trended higher in mice with KO bone marrow, but they were not statistically significant (Figure 5C). We also observed mortality in mice with WT marrow ($n = 3$ of 19) and none in those with KO marrow ($n = 0$ of 20). Overall, these findings demonstrate that leukocyte expression of MAP2K2 prolongs the duration of ALI and contributes to delayed bacterial clearance.

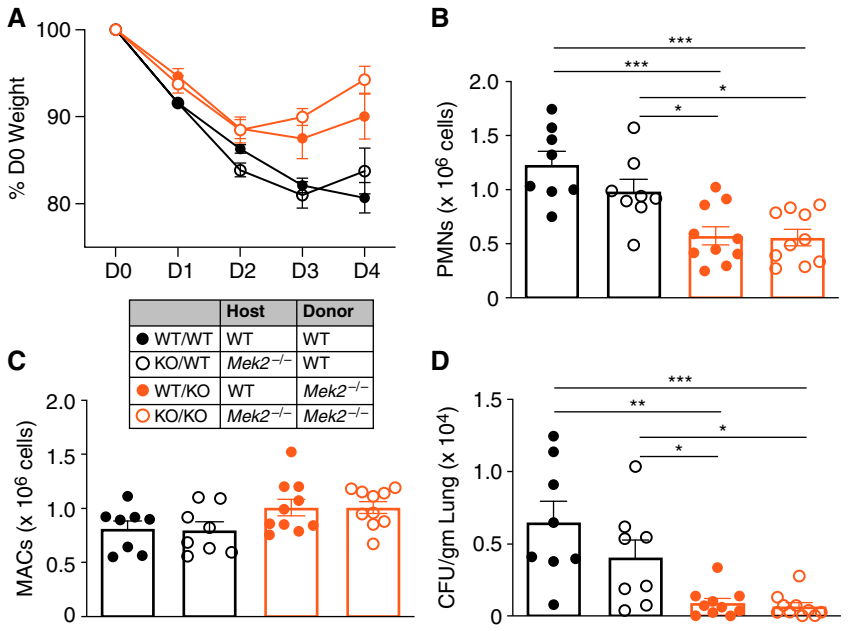

Figure 5. Leukocyte MAP2K2 delays recovery from PA ALI. Mice received PA via oropharyngeal aspiration and were harvested at D4. WT (solid circles) and knockout (KO) mice (open circles) received WT bone marrow (black) or KO bone marrow (red). (*A*) Mice with KO bone marrow (KO/KO and WT/KO) had earlier recovery of total body weight compared with those with WT bone marrow (WT/WT and KO/WT). (*B*) BAL neutrophils (PMNs) were lower in mice with KO bone marrow. (*C*) AM numbers were unaffected by genotype. (*D*) Bacterial cfu/g of lung were lower in mice with KO bone marrow. Analysis was performed using ANOVA, and data are presented as mean ± SEM ($n = 8$–20/group). $^{*}P < 0.05$, $^{**}P < 0.01$, and $^{***}P < 0.001$. MAC = alveolar macrophage.

Discussion

ARDS remains a significant problem in need of new pharmaceutical approaches to improve its resolution. In the pre–coronavirus disease (COVID-19) era, antiinflammatory approaches failed to improve outcomes (30–33), despite the findings that increased BAL neutrophils (34–37) and proinflammatory cytokines/chemokines, such as CXCL1 (CXC ligand 1)/IL-8 and CCL2/MCP-1 (monocyte chemoattractant protein–1) (38), associate with worse clinical outcomes. In those with COVID-19 requiring supplemental oxygen and/or mechanical ventilation, immunosuppressants, such as dexamethasone or IL-6 receptor antagonists, modestly improve outcomes, demonstrating that for specific causes of ARDS, antiinflammatory approaches may be therapeutic (39–41). With the surge of ARDS cases associated with COVID-19, there is an urgent need to understand novel pathways involved in resolution of lung inflammation and injury to provide the basis for new therapeutic approaches.

Increased activation of MAPK/ERK pathways has been reported in both murine ALI and human ARDS, suggesting shared mechanisms across species (7, 8). In murine models of sterile and infectious ALI, inhibitors to MAP2K1/MAP2K2 are beneficial in modifying the acute inflammatory response and promoting faster resolution (9, 10, 42). These findings suggest contributory roles for these kinases in promoting and sustaining lung inflammation. Although MAP2K1 and MAP2K2 are homologs and activate ERK1/2, they have distinct regulatory roles in ALI. In myeloid MAP2K1-deficient mice, we observed increased inflammatory cytokine expression, sustained inflammatory cell influx into the lung, and increased activation of the MAP2K2-ERK1/2 pathway (25). In contrast, *Mek2*$^{-/-}$ mice had faster resolution of lung inflammation and reduced activation of the MAP2K2-ERK1/2 pathway. One potential explanation for these disparate findings is that MAP2K1, but not MAP2K2, has an inhibitory site that can be phosphorylated by ERK1/2 in negative feedback loop (23). Hence, MAP2K1 may be required to deactivate MAP2K2 to promote ALI resolution.

Our studies in both myeloid MAP2K1-deficient mice (25) and MAP2K2 bone marrow chimeras suggest that sustained activation of MAP2K2 in myeloid cells is a key regulator of ALI duration. It remains to be determined if ALI duration is driven by MAP2K2 expressed by monocytes, macrophages, or neutrophils. In addition to regulating inflammatory and reparative programming by macrophages (10), MAPK/ERK pathways regulate cell survival and cell death pathways, including NETosis (24, 43, 44). Because delayed neutrophil apoptosis or increased NETosis may contribute to ALI severity and duration (45), it will be important to determine if MAP2K2 has a role in regulating these processes. Furthermore, because leukocyte MAP2K2 is the critical source, it will be important to assess the generalizability of a role of MAP2K2 in other models of ALI. In our unpublished studies, *Mek2*$^{-/-}$ mice have reduced neutrophilic lung inflammation in a short-term cigarette-smoke-exposure model, suggesting that these pathways may be relevant in other forms of lung injury.

By dissecting out the specific contribution of MAP2K2 in ALI, our murine studies demonstrate that MAP2K2 expression has no impact on the early recruitment of neutrophils to the alveolar compartment. However, in both sterile and infectious models of lung injury, the resolution was delayed in MAP2K2-sufficient mice. These MAP2K2-dependent pathways are highlighted by the transcriptional changes observed in the lung at Days 2 and 4 after ALI. On Day 2, transcriptional activation of inflammatory programming was present in both genotypes. However, in the small number of genes that were differentially expressed between genotypes at Day 2, inflammatory pathways were enriched in WT mice. These findings indicate that MAP2K2 is a small modifier of the initial inflammatory programming in PA ALI. By Day 4, *Mek2*$^{-/-}$ mice had enrichment of wound repair pathways, whereas WT mice continued to have greater enrichment of inflammatory pathways. These findings are consistent with the faster resolution of BAL

neutrophilia and vascular leak observed in *Mek2*$^{-/-}$ mice. Overall, the transcriptional and ALI measurements indicate that MAP2K2 is a critical regulator of ALI duration by sustaining inflammatory programming. One limitation of these transcriptional studies is that differences in inflammatory gene expression may reflect changes in the leukocyte composition in the lung. Future studies will require assessing MAP2K2-dependent transcriptional changes within sorted leukocyte populations.

MAP2K inhibitors, which have been developed as cancer therapeutics, target both isoforms. However, our findings indicate that MAP2K2 is the critical isoform to target in ALI. Our studies with MAP2K inhibitors demonstrate a benefit in murine models of ALI (9, 10), suggesting that short-term inhibition of MAP2K1 in lung injury is not deleterious if MAP2K2 activation is also blocked. However, the development of more selective inhibitors could allow for novel ALI therapeutics with less potential toxicity.

Given the heterogeneity of ARDS, the identification of biomarkers to identify ARDS subtypes may help guide more personalized therapeutics. Translating these findings to ARDS, we evaluated SNPs in *MAP2K1* and *MAP2K2* for association with ARDS susceptibility and ARDS mortality using the iSPAAR cohort. We identified an SNP in *MAP2K2* that associates with death in patients with ARDS. Future studies are needed to validate these findings in other cohorts and assess the association with MAP2K2 concentrations and the activation of its downstream pathways. Identifying patients who may benefit from inhibition of this pathway could prove a path forward in ARDS therapeutics. ■

Author disclosures are available with the text of this article at www.atsjournals.org.

Acknowledgment: The Genotype-Tissue Expression (GTEx) Project was supported by the Common Fund of the Office of the Director of the National Institutes of Health, and by the National Cancer Institute, National Human Genome Research Institute, National Heart, Lung, and Blood Institute (NHLBI), National Institute on Drug Abuse, National Institute of Mental Health, and National Institute of Neurological Disorders and Stroke, and some data used for the analyses described in this manuscript were obtained from: dbGaP accession number phs000424.vN.pN on 4/4/2019. Other datasets were obtained as part of the identification of SNPs Predisposing to Altered ALI Risk (iSPAAR) study funded by the NHLBI (RC2 HL101779).

References

1. Manicone AM. Role of the pulmonary epithelium and inflammatory signals in acute lung injury. *Expert Rev Clin Immunol* 2009;5:63–75.
2. Ware LB, Matthay MA. The acute respiratory distress syndrome. *N Engl J Med* 2000;342:1334–1349.
3. Fan E, Beitler JR, Brochard L, Calfee CS, Ferguson ND, Slutsky AS, *et al.* COVID-19-associated acute respiratory distress syndrome: is a different approach to management warranted? *Lancet Respir Med* 2020;8:816–821.
4. Pham T, Rubenfeld GD. Fifty years of research in ARDS: the epidemiology of acute respiratory distress syndrome. A 50th birthday review. *Am J Respir Crit Care Med* 2017;195:860–870.
5. Rubenfeld GD, Herridge MS. Epidemiology and outcomes of acute lung injury. *Chest* 2007;131:554–562.
6. Zambon M, Vincent JL. Mortality rates for patients with acute lung injury/ARDS have decreased over time. *Chest* 2008;133:1120–1127.
7. Moore BB. Groundhog day for rodent models of acute lung injury: clear relevance or renewed debate? *Am J Respir Cell Mol Biol* 2017;57:141–142.
8. Sweeney TE, Lofgren S, Khatri P, Rogers AJ. Gene expression analysis to assess the relevance of rodent models to human lung injury. *Am J Respir Cell Mol Biol* 2017;57:184–192.
9. Long ME, Gong KQ, Eddy WE, Liles WC, Manicone AM. Pharmacologic inhibition of MEK1/2 reduces lung inflammation without impairing bacterial clearance in experimental *Pseudomonas aeruginosa* pneumonia. *Pneumonia (Nathan)* 2017;9:13.
10. Long ME, Eddy WE, Gong KQ, Lovelace-Macon LL, McMahan RS, Charron J, *et al.* MEK1/2 inhibition promotes macrophage reparative properties. *J Immunol* 2017;198:862–872.
11. Chen S, Xu H, Ye P, Wu C, Ding X, Chen S, *et al.* Trametinib alleviates lipopolysaccharide-induced acute lung injury by inhibiting the MEK-ERK-Egr-1 pathway. *Int Immunopharmacol* 2020;80:106152.
12. Caunt CJ, Sale MJ, Smith PD, Cook SJ. MEK1 and MEK2 inhibitors and cancer therapy: the long and winding road. *Nat Rev Cancer* 2015;15:577–592.
13. Curjuric I, Imboden M, Nadif R, Kumar A, Schindler C, Haun M, *et al.* Different genes interact with particulate matter and tobacco smoke exposure in affecting lung function decline in the general population. *PLoS ONE* 2012;7:e40175.
14. Pelaia C, Vatrella A, Crimi C, Gallelli L, Terracciano R, Pelaia G. Clinical relevance of understanding mitogen-activated protein kinases involved in asthma. *Expert Rev Respir Med* 2020;14:501–510.
15. Neuzillet C, Tijeras-Raballand A, de Mestier L, Cros J, Faivre S, Raymond E. MEK in cancer and cancer therapy. *Pharmacol Ther* 2014;141:160–171.
16. Rose BA, Force T, Wang Y. Mitogen-activated protein kinase signaling in the heart: angels versus demons in a heart-breaking tale. *Physiol Rev* 2010;90:1507–1546.
17. Bos LDJ, Scicluna BP, Ong DSY, Cremer O, van der Poll T, Schultz MJ. Understanding heterogeneity in biologic phenotypes of acute respiratory distress syndrome by leukocyte expression profiles. *Am J Respir Crit Care Med* 2019;200:42–50.
18. Shi-Lin D, Yuan X, Zhan S, Luo-Jia T, Chao-Yang T. Trametinib, a novel MEK kinase inhibitor, suppresses lipopolysaccharide-induced tumor necrosis factor (TNF)-α production and endotoxin shock. *Biochem Biophys Res Commun* 2015;458:667–673.
19. Li P, Wu Y, Li M, Qiu X, Bai X, Zhao X. AS-703026 inhibits LPS-induced TNFα production through MEK/ERK dependent and independent mechanisms. *PLoS ONE* 2015;10:e0137107.
20. Smith JA, Mayeux PR, Schnellmann RG. Delayed mitogen-activated protein kinase/extracellular signal-regulated kinase inhibition by trametinib attenuates systemic inflammatory responses and multiple organ injury in murine sepsis. *Crit Care Med* 2016;44:e711–e720.
21. Scholl FA, Dumesic PA, Barragan DI, Harada K, Bissonauth V, Charron J, *et al.* Mek1/2 MAPK kinases are essential for mammalian development, homeostasis, and Raf-induced hyperplasia. *Dev Cell* 2007;12:615–629.
22. Bissonauth V, Roy S, Gravel M, Guillemette S, Charron J. Requirement for Map2k1 (Mek1) in extra-embryonic ectoderm during placentogenesis. *Development* 2006;133:3429–3440.
23. Roskoski R Jr. MEK1/2 dual-specificity protein kinases: structure and regulation. *Biochem Biophys Res Commun* 2012;417:5–10.
24. Zmajkovicova K, Jesenberger V, Catalanotti F, Baumgartner C, Reyes G, Baccarini M. MEK1 is required for PTEN membrane recruitment, AKT regulation, and the maintenance of peripheral tolerance. *Mol Cell* 2013;50:43–55.
25. Long ME, Gong KQ, Eddy WE, Volk JS, Morrell ED, Mikacenic C, *et al.* MEK1 regulates pulmonary macrophage inflammatory responses and resolution of acute lung injury. *JCI Insight* 2019;4:e132377.
26. Catalanotti F, Reyes G, Jesenberger V, Galabova-Kovacs G, de Matos Simoes R, Carugo O, *et al.* A Mek1-Mek2 heterodimer determines the strength and duration of the Erk signal. *Nat Struct Mol Biol* 2009;16:294–303.
27. ARDSnet and the iSPAAR Consortium: genomic basis of susceptibility and outcomes in patients with the acute respiratory distress syndrome

(ARDS): dbGaP study accession phs000631.v1.p1. Bethesda, MD: National Heart, Lung, and Blood Institute; 2014 [accessed 2019 Apr 22]. Available from: http://www.ncbi.nlm.nih.gov/projects/gap/cgi-bin/study.cgi?study_id=phs000631.v1.p1.
28. Bélanger LF, Roy S, Tremblay M, Brott B, Steff AM, Mourad W, *et al.* Mek2 is dispensable for mouse growth and development. *Mol Cell Biol* 2003;23:4778–4787.
29. GTEx Portal. Cambridge, MA: Broad Institute of MIT and Harvard [accessed 2019 Apr 4]. Available from: https://gtexportal.org/home/.
30. Tonelli AR, Zein J, Adams J, Ioannidis JP. Effects of interventions on survival in acute respiratory distress syndrome: an umbrella review of 159 published randomized trials and 29 meta-analyses. *Intensive Care Med* 2014;40:769–787.
31. Steinberg KP, Hudson LD, Goodman RB, Hough CL, Lanken PN, Hyzy R, *et al.*; National Heart, Lung, and Blood Institute Acute Respiratory Distress Syndrome (ARDS) Clinical Trials Network. Efficacy and safety of corticosteroids for persistent acute respiratory distress syndrome. *N Engl J Med* 2006;354:1671–1684.
32. Iwata K, Doi A, Ohji G, Oka H, Oba Y, Takimoto K, *et al.* Effect of neutrophil elastase inhibitor (sivelestat sodium) in the treatment of acute lung injury (ALI) and acute respiratory distress syndrome (ARDS): a systematic review and meta-analysis. *Intern Med* 2010;49: 2423–2432.
33. Adhikari N, Burns KE, Meade MO. Pharmacologic therapies for adults with acute lung injury and acute respiratory distress syndrome. *Cochrane Database Syst Rev* 2004;2004(4):CD004477.
34. Steinberg KP, Milberg JA, Martin TR, Maunder RJ, Cockrill BA, Hudson LD. Evolution of bronchoalveolar cell populations in the adult respiratory distress syndrome. *Am J Respir Crit Care Med* 1994;150: 113–122.
35. Williams AE, Chambers RC. The mercurial nature of neutrophils: still an enigma in ARDS? *Am J Physiol Lung Cell Mol Physiol* 2014; 306:L217–L230.
36. Groeneveld AB, Raijmakers PG, Hack CE, Thijs LG. Interleukin 8-related neutrophil elastase and the severity of the adult respiratory distress syndrome. *Cytokine* 1995;7:746–752.
37. Baughman RP, Gunther KL, Rashkin MC, Keeton DA, Pattishall EN. Changes in the inflammatory response of the lung during acute respiratory distress syndrome: prognostic indicators. *Am J Respir Crit Care Med* 1996;154:76–81.
38. Rosseau S, Hammerl P, Maus U, Walmrath HD, Schütte H, Grimminger F, *et al.* Phenotypic characterization of alveolar monocyte recruitment in acute respiratory distress syndrome. *Am J Physiol Lung Cell Mol Physiol* 2000;279:L25–L35.
39. Horby P, Lim WS, Emberson JR, Mafham M, Bell JL, Linsell L, *et al.*; RECOVERY Collaborative Group. Dexamethasone in hospitalized patients with COVID-19. *N Engl J Med* 2021;384:693–704.
40. Gordon AC, Mouncey PR, Al-Beidh F, Rowan KM, Nichol AD, Arabi YM, *et al.*; REMAP-CAP Investigators. Interleukin-6 receptor antagonists in critically ill patients with COVID-19. *N Engl J Med* 2021;384:1491–1502.
41. Marconi VC, Ramanan AV, de Bono S, Kartman CE, Krishnan V, Liao R, *et al.*; COV-BARRIER Study Group. Efficacy and safety of baricitinib for the treatment of hospitalised adults with COVID-19 (COV-BARRIER): a randomised, double-blind, parallel-group, placebo-controlled phase 3 trial. *Lancet Respir Med* 2021;9:1407–1418.
42. Schuh K, Pahl A. Inhibition of the MAP kinase ERK protects from lipopolysaccharide-induced lung injury. *Biochem Pharmacol* 2009;77: 1827–1834.
43. Lu Z, Xu S. ERK1/2 MAP kinases in cell survival and apoptosis. *IUBMB Life* 2006;58:621–631.
44. Hakkim A, Fuchs TA, Martinez NE, Hess S, Prinz H, Zychlinsky A, *et al.* Activation of the Raf-MEK-ERK pathway is required for neutrophil extracellular trap formation. *Nat Chem Biol* 2011;7:75–77.
45. Potey PM, Rossi AG, Lucas CD, Dorward DA. Neutrophils in the initiation and resolution of acute pulmonary inflammation: understanding biological function and therapeutic potential. *J Pathol* 2019;247:672–685.